EFDA–JET–CP(10)05/21

Henning Thomsen, Thomas Eich, Stéphane Devaux, Elena de la Luna,
Gilles Arnoux, Wojtek Fundamenski, Albrecht Herrmann,
Gabriella Saibene, Roberta Sartori, and JET EFDA Contributors

Analysis of ELM-resolved power fluxes in JET ripple discharges

Analysis of ELM-resolved power fluxes in JET ripple discharges

Henning Thomsen[1,*], Thomas Eich[1], Stéphane Devaux[1,2], Elena de la Luna[1,3], Gilles Arnoux[2], Wojtek Fundamenski[2], Albrecht Herrmann[1], Gabriella Saibene[4], Roberta Sartori[4], and JET EFDA Contributors*

JET-EFDA, Culham Science Centre, OX14 3DB, Abingdon, UK

EURATOM/UKAEA Fusion Association, Culham Science Centre, Abingdon OX14 3DB, UK.
[1]Max-Planck-Institut für Plasmaphysik, EURATOM-Association, D-17491, Greifswald, Germany.
[2]EURATOM/UKAEA Fusion Association, Culham Science Centre, Abingdon OX14 3DB, UK.
[3]Association EURATOM-CIEMAT, Avda Complutense – Madrid, Spain
[4]FUSION FOR ENERGY Joint Undertaking, 08019 Barcelona, Spain.
** See annex of F. Romanelli et al, "Overview of JET Results",*
(Proc. 22 nd IAEA Fusion Energy Conference, Geneva, Switzerland (2008)).

Preprint of Paper to be submitted for publication in Proceedings of the
19th International Conference on Plasma Surface Interactions, San Diego, California, USA.
(24th May 2010 - 28th May 2010)

ABSTRACT

One critical factor in the standard H-mode scenario of the ITER operation is the maximum allowable energy density onto the plasma facing components. Especially the transient impact of Edge Localized Modes (ELMs) onto the divertor target plates must stay below an energy density of 0.5 MJ/m^2 within 0.5ms. Results from ELM-resolved IR-measurements of the divertor target at the JET tokamak are presented. The effect of gas fueling on the transient divertor target load by ELMs in a magnetic configuration with natural TF ripple ($\delta_{BT}=0.08\%$) and a configuration in ITER-like ripple ($\delta_{BT}=0.50\%$) are investigated. It is found, that gas fueling reduces the ELM size in the pedestal and the ELM power arriving at the divertor target. ELM power broadening with increasing ELM size is observed. The divertor target ELM energy density decreases for increasing gas fueling with $\delta_{BT}=0.50\%$ but is increasing for a gas scan with $\delta_{BT}=0.08\%$.

1. INTRODUCTION

The divertor target life time is determined by/related to transient and stationary heat loads. Transient heat loads are mainly caused by disruptions and ELMs, whereas the stationary heat loads are determined by the inter-ELM transport in the scrape-off layer. Based on scaling assumptions, the heat loads of present day devices are extrapolated to the expected ITER values. The extrapolation of transient heat loads is of special concern, especially due to the lack of a reliable model for ELM power load scaling.

The material erosion limit depends on the value for the transient energy density as well as the temporal shape of the ELM. For the ITER divertor targets a threshold energy density of $\varepsilon=0.5$MJ/m^2 for ELMs with a shape with a 0.25 ms rise time and a fall time between 0.25ms and 0.5ms [1]. From the present knowledge, the expected natural ELM size in ITER for the intended plasma heating and confinement (ELMy H-mode) would lead to serious erosion of the divertor target and thus limit the divertor life time [1]. ELM mitigation techniques are under survey to decrease the ELM size, e.g. increased fueling, vertical kicks and magnetic perturbation fields.

The discrete number and size of toroidal magnetic field coils introduces toroidally periodic perturbation of the magnetic field, the toroidal field (TF) ripple. It can be quantified by $\delta_{BT}=(B_{max}-B_{min})/(B_{max}+B_{min})$ for maximum values at the separatrix. The coil configuration of ITER will lead to a Toroidal Field (TF) ripple in the order of $\delta_{BT}=0.50$ % (with ferritic inserts to reduce the ripple) [2]. It was found, that an increased TF ripple is associated with confinement degradation, density pump-out and increased ELM frequency.

The experiments presented in the scope of this paper aim at an improved understanding of the effect of TF ripple on ELM target loads and comprise two gas fueling scans conducted in JET, one in a magnetic configuration with natural TF ripple ($\delta_{BT}=0.08\%$) and the other in a configuration in ITER-like ripple ($\delta_{BT}=0.50\%$).

2. RESULTS FROM JET RIPPLE EXPERIMENTS

In JET it is possible to increase the TF ripple by powering odd and even TF coils in two sets and applying different currents to the two coil sets. In recent experiments, the TF ripple was thereby

increased from $\delta_{BT} = 0.08\%$ (the natural ripple level in JET) to $\delta_{BT} = 1\%$. Enhanced fast ion losses leading to alpha-ion losses of the order of 1% are observed, but are of no concern for the fast ion confinement. The plasma density is found to decrease with increasing δ_{BT}, which is in general referred to as density pump-out. The pump-out is not proportional to fast ion losses [3]. The electron temperature remains approximately constant, whereas the ion temperature increases. In terms of stored energy, the density loss is not completely compensated by the ion temperature increase and the stored energy decreases by up to 20% at maximum TF ripple of $\delta_{BT} = 1\%$ for approximately constant net input power. Most of the stored energy loss with respect to the natural TF ripple case is already observed for $\delta_{BT} = 0.50\%$. It is found that the plasma confinement is continuously decreasing with increasing TF ripple, when the gas fueling is kept constant [3]. Another feature of ripple discharges is the slow-down of toroidal plasma rotation, which is observed to change direction in the plasma edge for $\delta_{BT} = 1.0\%$ [4].

3. METHODS

After the installation of a new fast Infra Red (IR) camera at JET [6], experiments were carried out to quantify the effect of TF ripple on the divertor power loads. The magnetic configuration was optimized for the IR view in these experiments with the outer strike line on tile 5 of the high heat flux divertor. The high spatial and temporal resolution of the IR camera allows for ELM resolved measurements of temperature profiles with a good spatial resolution of 1.7 mm per pixel and a time resolution of 86 μs. An improved version of the THEODOR code was used to calculate the heat fluxes assuming a 2d geometry and temperature dependent material parameters [7]. The data is divided into ELM and inter-ELM phases and the power on the divertor target and the wetted area ($A = P/Q$, P: power [W], Q: peak heat flux [W/m^2]) is estimated for each Elm and inter-ELM phase. The ELM energy densities ($E = \int Q dt$) are calculated for a poloidal average of 1 cm centered around the position of the ELM peak location. The integration time is from the ELM start (steep increase of heat flux) until the 1/e decay after the ELM peak.

4. RESULTS

A series of discharges ($B_t = 2.3$T, $I_p = 2.6$Ma, $q_{95} = 3.1$, $P_{NBI} = 15$-16MW, low triangularity shape) with type-I ELMy H-mode was conducted. Three gas fueling rates (0, 6 and 11×10^{21} el/s) during the H-mode phase and three TF ripple values ($\delta_{BT} = 0.08\%$, $\delta_{BT} = 0.50\%$) were changed on a pulse by pulse basis, resulting in a data base of 6 discharges to be described in the remains of this paper. In the natural TF ripple discharges, an increase of gas fueling leads to a reduction in the pedestal energy loss per ELM (W_{ELM}, the ELM size). The ELM frequency increases from 23Hz to 43Hz for the intermediate gas fueling rate and drops to 33Hz for the highest applied fueling rate in this scan. The peak power during an ELM is found to increase linearly with increasing ELM size (Fig.1a). The inter-ELM power shows a slight decrease with ELM size from approximately 3MW (400kJ ELM size) to 2MW (100kJ). The ELM-wetted area displays a similar trend (Fig.1b): the ELM power shows a mean broadening from 0.5m^2 for 100kJ ELM size to 1.2 m^2 for 400kJ ELM size. The inter-ELM wetted area is almost constant at 0.3m^2 (calculated inter-ELM wetted areas larger

than the ELM-wetted areas are caused by the very low amplitudes in the heat fluxes and powers, see next section), whereas the ELM wetted area shows a mean broadening from 0.5m² for 100kJ ELM size to 1.2m² for 400 kJ ELM size. The maximum observed ELM energy densities, plotted in Fig.1c, are slightly increasing with decreasing ELM size.

In the gas fueling scan in discharges with $\delta_{BT} = 0.50\%$ the 250kJ ELMs show a peak power of 80MW with a wetted area of 1m² and 60MW for 150kJ ELMs with a wetted area of 0.8m². The inter-ELM power remains constant at approximately 0.3m² and 3MW power in the range from 100kJ to 300kJ. The ELM frequency decreases slightly with increasing gas fueling from 31Hz over 31Hz to 27Hz.

In Fig.2, the histograms of the ELM energy density distribution are shown for the two gas fueling scans with different TF ripple. For $\delta_{BT} = 0.08\%$ the estimated maximum ELM energy density is increasing with increasing gas fueling, whereas for the $\delta_{BT} = 0.50\%$ gas scan the opposite trend is found. These results are summarized in Fig.3, where the number of ELMs with a minimum energy density E*>33kJ/m² (80% of the ELMs have a smaller energy densities in the reference discharge, with $\delta_{BT} = 0.08\%$ and no gas fueling) is plotted versus the H-mode confinement factor, H_{98}.

In Fig. 4 the ratio of the energy density distributions during ELM rise and fall time are plotted versus the rise time. Gas fueling in $\delta_{BT} = 0.08\%$ pulses leads to longer ELM rise times. For these, the energy density in the rise phase is larger than in the tail. For the pulses with $\delta_{BT} = 0.5\%$ the rise time is longer by ~100s (IR frame time: 86) compared to data from $\delta_{BT} = 0.08$ % pulse without gas fueling.

5. DISCUSSION

We note here, that due to the limited spatial resolution on the inboard divertor side, the analysis of inboard outboard asymmetries of the ELM power deposition is challenging. Here, we focus on data from the divertor outboard side.

The inter-ELM wetted area is relatively constant at about 0.3m² over a wide range of different ELM sizes, if we consider the inter-ELM wetted areas which are larger than the ELM-wetted areas ($W_{ELM} < 150$kJ) being caused by diagnostics limitations. The accuracy of the heat flux calculation is rather limited for discharge conditions with low target temperatures by the diagnostics sensitivity, which leads to large errors in the wetted area calculation. Considering flux expansion (5.5) and divertor circumfence (17.2m), the inter-ELM wetted area can be mapped to an outer mid-plane integral power width of approximately $\lambda_q = 3.5$mm. Previous studies in JET report the smallest width to be approximately $\lambda_q = 5$mm [10].

The observed ELM power broadening with ELM size in JET is favorable in terms of divertor target life time with larger ELMs, since the power is spread over a larger area. This large ELM power broadening was first discovered in IR data from a ripple scan [5] but seems to be an universal feature in JET H-modes [6]. For ITER, a similar power broadening might ease the requirements on the ELM sizes compatible with a sufficiently long divertor life time.

The relation between ELM size in the pedestal and ELM energy density at the target is not well understood for JET plasmas. This has also consequences for the assessment of the success of ELM

mitigation techniques (like gas fueling, EFCC, etc., cf. [8]), which are sometimes evaluated based on the ELM size and ELM frequency only. Gas fueled H-modes show a smaller ELM size at higher ELM frequency and the confinement degrades. The loss of energy confinement with increasing density, as shown in Fig.3, is within the uncertainties in agreement with the IPB98(y,2) scaling, $H_{98} = \tau_E/\tau_{E,IPB98} \sim n^{-0.4}$ [9]. If we assume an H-mode with a fraction of ELMs with an energy density above the threshold for target erosion, any increase in ELM frequency due to an applied mitigation technique just reducing the (pedestal) ELM size but leaving the ELM energy densities constant will have serious consequences for the divertor target life time. For the two gas fueling scans with different TF ripple, the ELM energy densities at the target scale differently: additional gas fueling for $\delta_{BT} = 0.50\%$ reduces the number of ELMs with a high energy density, whereas the opposite trend, an increase of the number of ELMs with a high energy, is found for additional gas fueling in H-mode with natural TF ripple. The general trends could be confirmed for a further gas fueling scan in natural TF ripple H-mode as well as for a gas fueling scan in a series of discharges with $\delta_{BT} = 0.75\%$.

The divertor target life time is a function of the number of ELMs with an energy density above the material erosion threshold. For ITER the threshold is $\varepsilon^* = 0.5$ MJ/m^2 for a certain temporal shape of the ELM power on the target [1]. The temporal shape of the ELM power load is important for the characterization of the energy density limit. The frame time of the JET IR camera is marginally capable to resolve changes in the ELM rise time. The observed rise times (~200 - 500s) are also expected for ELMs in ITER. The ratio between rise and fall energy density shows no large difference for the two gas scans, with the exception that ELMs with long rise times in the $\delta_{BT} = 0.08\%$ gas scan are more frequent. Further studies are needed for a better understanding of these findings and their extrapolation to ITER.

CONCLUSION

The JET experiments show a detrimental effect on the plasma confinement and the density for an increased TF ripple. The density pump-out can be compensated by increased gas fueling, however at the expense of the confinement quality. The ELM size is reduced by TF ripple increase as well as gas fueling and the ELM frequency increases. It is found in ELM resolved IR measurements, that the deposited power on the outboard divertor increases linear with the ELM size. The wetted area increases with the ELM size, whereas the inter-ELM wetted area stays constant. We observe an increasing ELM power broadening with ELM size. Divertor target erosion occurs for transient events with an energy density over a certain threshold. In a gas fueling scan in JET with a TF ripple comparable to the ITER value, the energy density is found to decrease with increasing fueling rate. The opposite behavior, an increase of the energy density with increasing fueling rate, is found for the low natural TF ripple in JET. A better understanding of the scaling of the ELM energy density with pedestal parameters is required to extrapolate these findings to ITER.

ACKNOWLEDGEMENTS

This work was supported by EURATOM and carried out within the framework of the European

Fusion Development Agreement. The views and opinions expressed herein do not necessarily reflect those of the European Commission.

REFERENCES

[1]. G. Federici et al. Plasma Physics Contribution Fusion **45** (2003) 1523, A. Loarte et al., Nuclear Fusion **47** (2007) S203.

[2]. A. Portone et al, Fusion Energy Design **83** (2008) 1619.

[3]. G. Saibene, R. Sartori et al., ECA 31F, (2007) O-4.001, G. Saibene et al., IAEA (2008) IT/EX2

[4]. P.C. de Vries et al. Plasma Physics Control Fusion **50** (2008) 065008

[5]. H. Thomsen et al., ECA 33E, (2009) P2.164

[6]. T. Eich et al., this conference

[7]. A. Herrmann et al., ECA 25 (2001) P

[8]. S. Jachmich et al., this conference

[9]. ITER Physics Basis, Nuclear Fusion **39** (1999) 2175

[10]. W. Fundamenski, J. Nuclear Material **390-391** (2009) 10

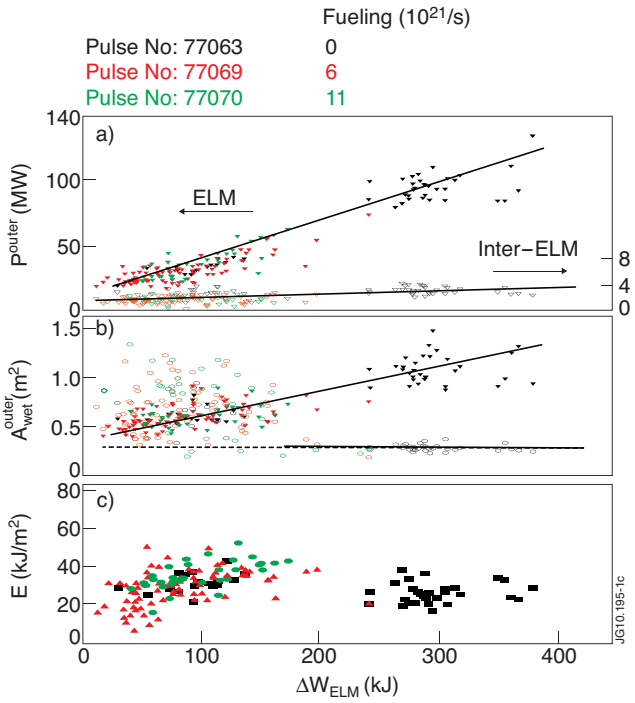

Figure 1: (a) Power on outboard divertor target estimated from IR camera measurements at ELM peaks (filled symbols) and inter-ELM phases (open symbols) for three discharges with δ_{BT} = 0.08 % and gas fueling during H-mode phase of 0 (black), 6×10^{21}el/s (red) and 11×10^{21}el/s (green). (b) Wetted area during ELMs (filled symbols) and inter-ELM phases (open symbols). The scatter in the wetted area for small ELM sizes (W_{ELM} < 150kJ) is mainly due to the small peak heat flux and power, which are at the dynamics resolution limit of the IR camera. (c) ELM energy density. Lines are plotted to guide the eye.

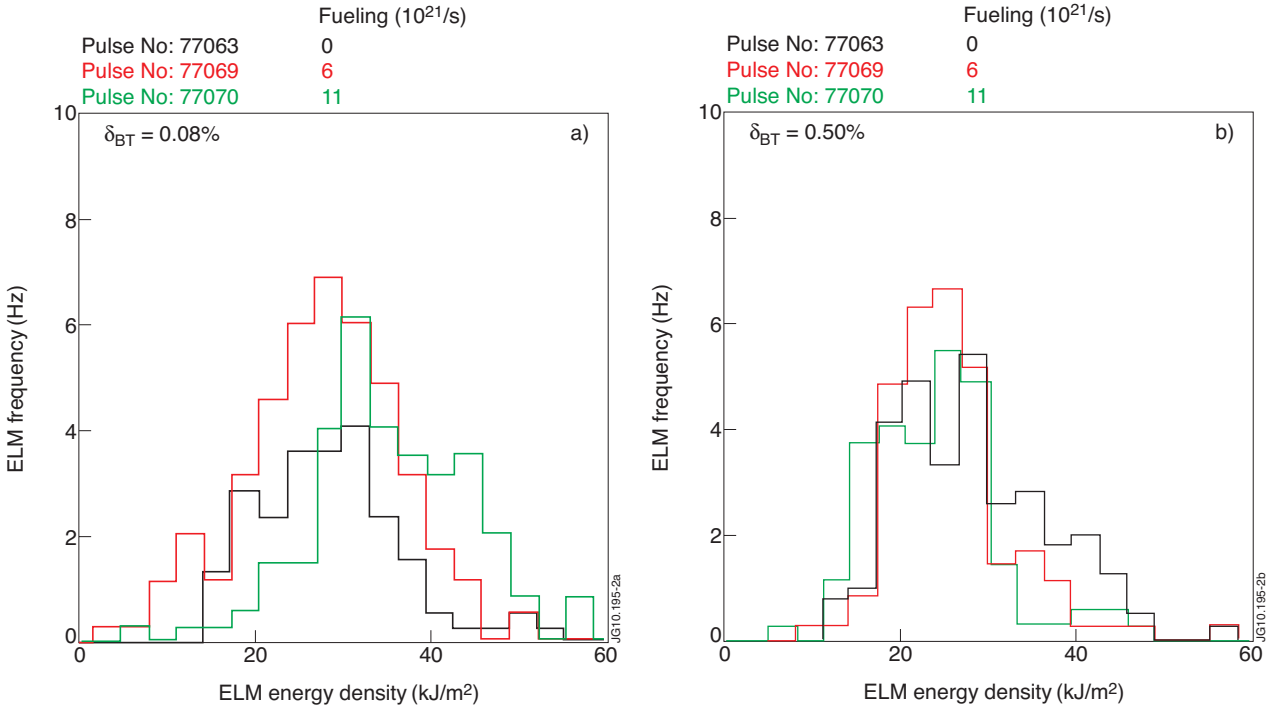

Figure 2: Histograms of the ELM energy density distribution for two gas fueling scans in (a): $\delta_{BT} = 0.08\%$ and (b) $\delta_{BT} = 0.50\%$.

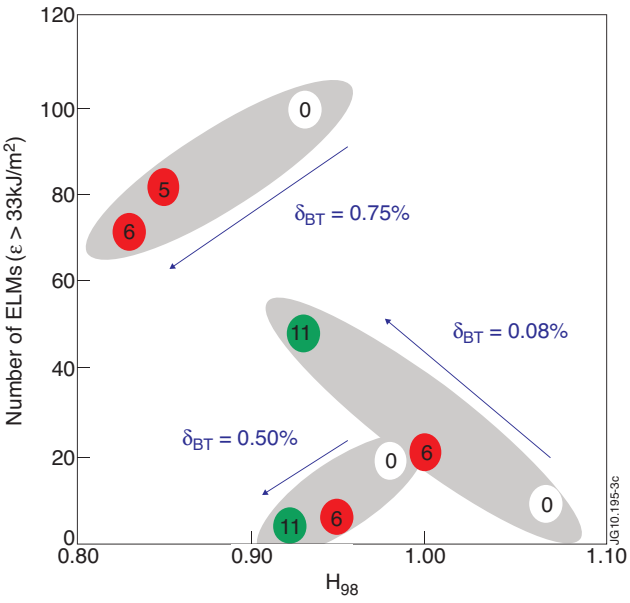

Figure 3: Number of ELMs with an energy density over a threshold of 33kJ/m^2 versus H-mode confinement factor H_{98} for three gas fueling scans (tree pulses each) with δ_{BT} = 0.08%, 0.50% and 0.75%. The number in circles denotes the gas fueling rate in 10^{21} el/s.

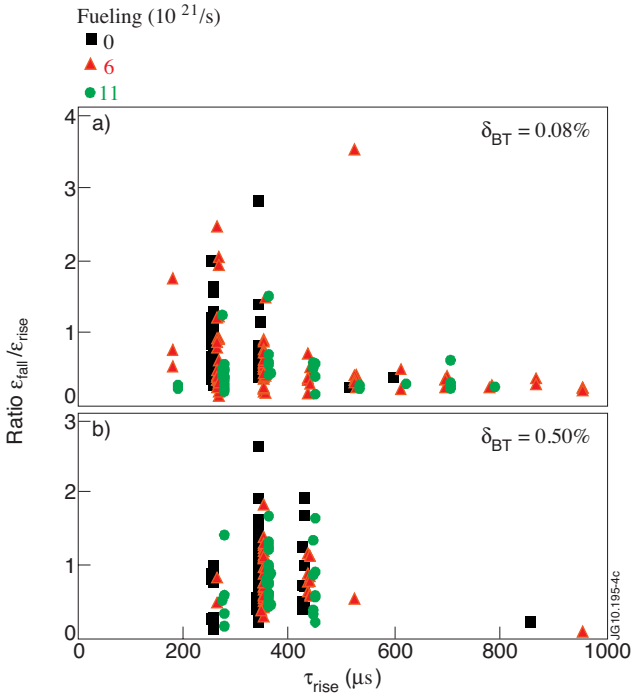

Figure 4: Ratio of the energy density distributions during ELM rise and fall time versus the rise time for (a) gas scan series in $\delta_{BT} = 0.08\%$ and (b) gas scan series in δ_{BT} = 0.50%. Colors denote the fueling rate. The data from different pulses have a small artificial offset in τ to improve the visibility in the plot.